Electronic Supplementary Material (ESI) for Chemical Communications

Theoretical studies of the mechanism of catalytic hydrogen production by a cobaloxime

James T. Muckerman,* and Etsuko Fujita

Electronic Supplementary Information

Table of Contents

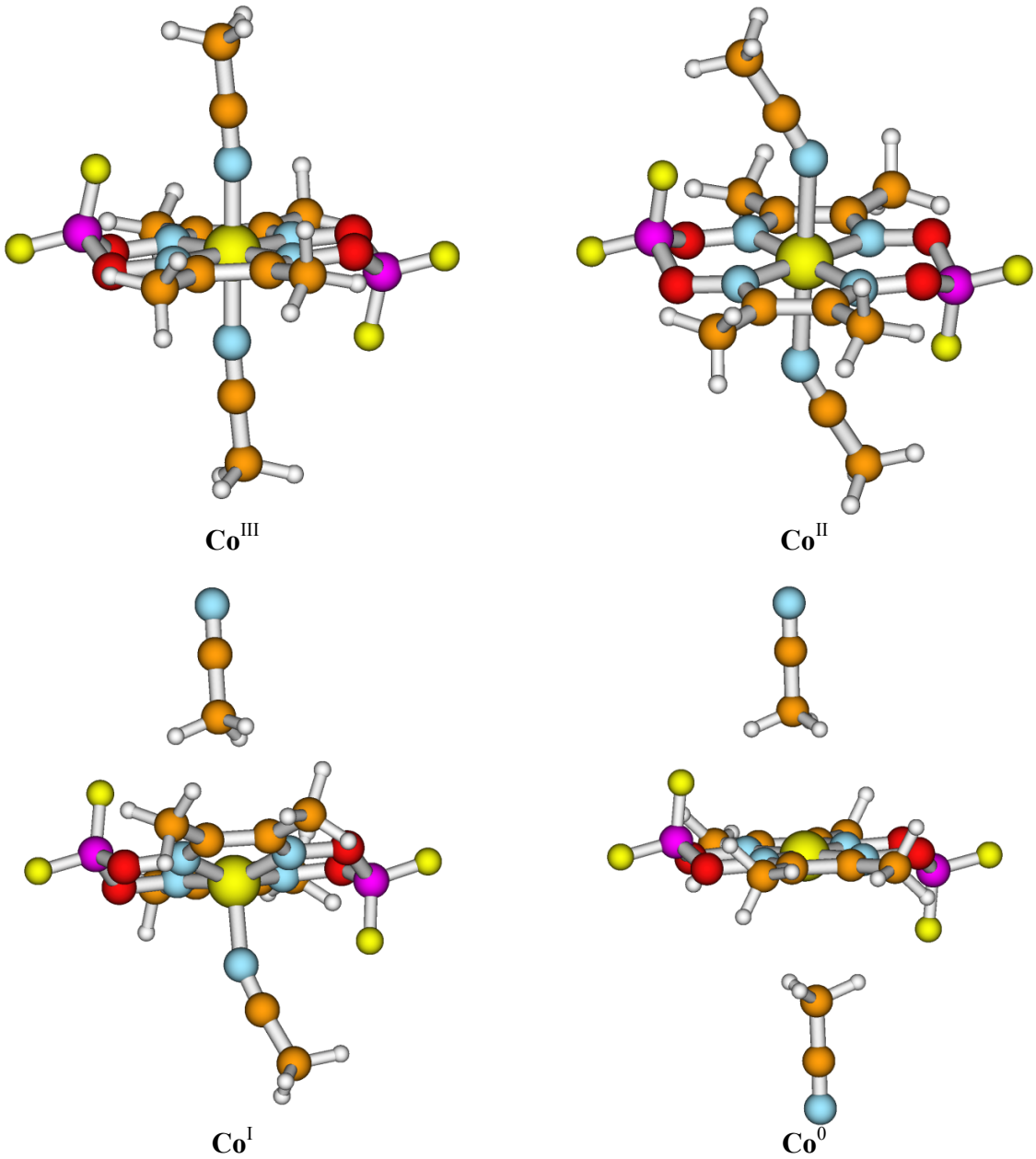

Fig. S1. Calculated structures of various oxidation states of $[Co^{II}(dmgBF_2)_2{\cdot}2CH_3CN]^0$, designated **Co**^{II}.

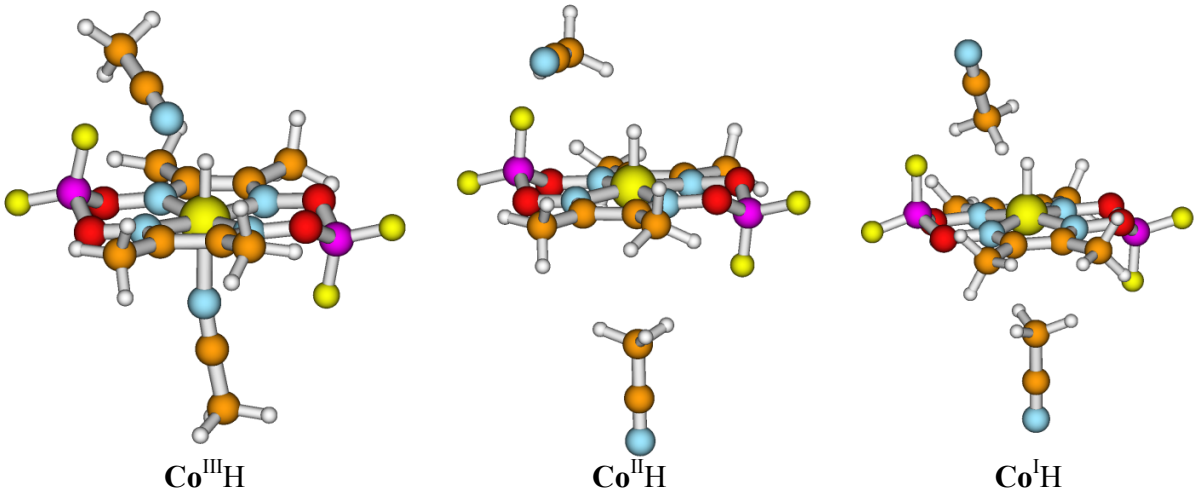

Fig. S2. Calculated structures of various oxidation states of $[Co^{III}H(dmgBF_2)_2{\cdot}2CH_3CN]^0$, designated **Co**^{III}H.

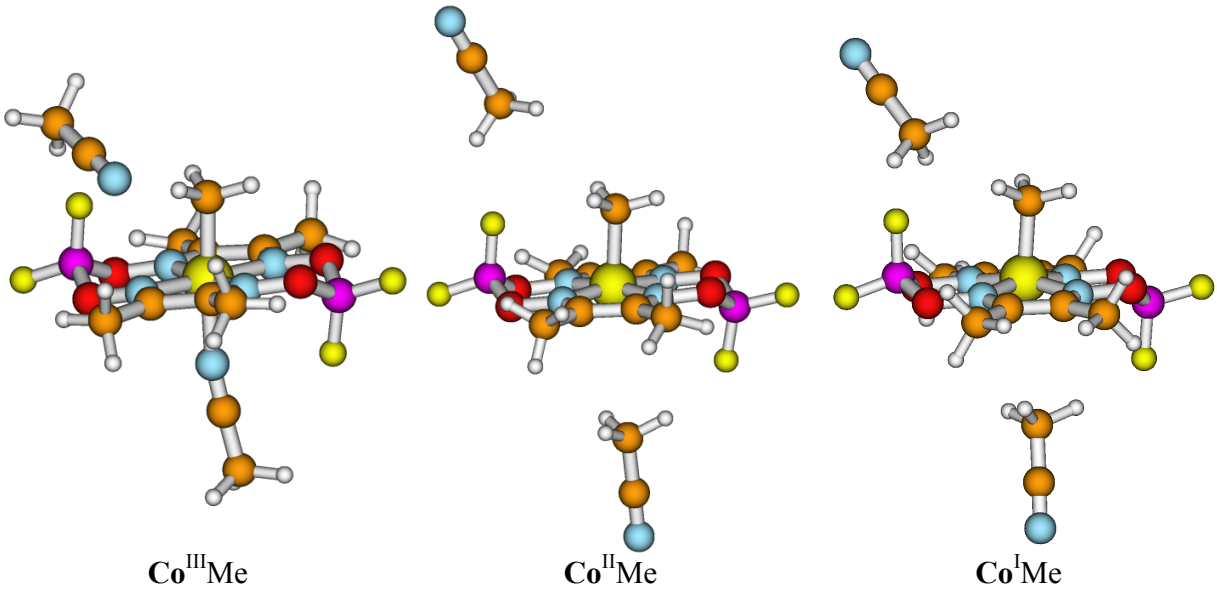

Fig. S3. Calculated structures of various oxidation states of $[Co^{III}CH_3(dmgBF_2)_2{\cdot}2CH_3CN]^0$, designated **Co**^{III}Me.

Details of the electronic structure calculations.

All computations were carried out with the Gaussian03 suite of programs[1] using the B3LYP hydrid density functional method.[2] All-electron basis sets were employed at the B3LYP/6-311++G(d,p)[3-6] // B3LYP/6-31+G(d,p)[7-9] 5d level of theory. Geometry optimizations and vibrational frequency calculations of all species were carried out with the smaller basis in the gas phase, and $\Delta G^{o}_{ZPE\&Th(g)}$ (the gas-phase zero-point energy and thermal corrections to the electronic energy) was calculated as the difference between the gas-phase free energy, $G^{o}_{(g)}$, and the optimized electronic energy, $E_{el,sm(g)}$. For species that do not have a gas-phase standard state, the geometry was re-optimized in a CPCM[10-12] treatment of the acetonitrile solvent using Bondi radii[13] with OFAC = 0.8 and RMIN = 0.5 to obtain the "total free energy in solution with all non-electrostatic terms", $G^{o}_{anest(s)} = E_{el,sm(g)} + \Delta G^{o}_{s,}$ to which $\Delta G^{o}_{ZPE\&Th(g)}$ is added to obtain the absolute free energy in solution, $G^{o}_{sm(s)}$, corresponding to a standard state of 1 atm. Here we do not make the standard state correction from one atm pressure in the gas phase to one molar in solution, $\Delta G^{o\rightarrow *} = 1.894$ kcal/mol,[14] because it would occur in the same number of species in the reactants and products of all reactions considered, and would cancel. Finally, a single-point electronic energy calculation at the gas-phase optimized geometry was carried out with the larger basis to obtain $E_{el,lg(g)}$, and the absolute free energy in solution was recalculated as $G^{*}_{lg(s)} = G^{*}_{sm(s)} + E_{el,lg(g)} - E_{el,sm(g)}$. We employed values of $G^{*}(H^{+}_{(s)}) = -266.5$ kcal/mol[14] and $G^{o}(e^{-}_{(g)}) = -0.868$ kcal/mol[15] recommended in the literature, and referenced all calculated reduction potentials to the normal hydrogen electrode (NHE), which we calculated from $G^{o}(e^{-}_{(g)})$, $G^{*}(H^{+}_{(s)})$ and $G^{o}(H_{2(g)})$ to be 4.474 V. Our calculated value for the absolute potential of the ferrocenium/ferrocene couple in acetonitrile is 4.972 V. For accurate comparisons of the relative energetics of various **Co** species, two explicit molecules of the acetonitrile solvent were included in the calculation for 6-, 5- and 4-coordinate complexes (Fig. 1). The calculated structures of a variety of formal oxidation states of **Co**, **Co**H and **Co**Me species considered here are shown in Figs. S1, S2 and S3, respectively, of this ESI.

All values of E^{o} and pK_a reported in this work were directly calculated from differences of absolute standard free energies of the individual species in the reactions being considered. No isodesmic schemes were employed to improve agreement between the calculated and experimental values. This said, we note that our calculated values of pK_{a1} (4.47) and pK_{a2} (13.62) are considerably lower than the values reported by Baffert et al.[16] (13.3 and 23.0, respectively) from simulations of experimental CV data, but our calculated $pK_{a2} - pK_{a1}$ differs by only 0.5 pH unit from their corresponding value. Therefore an isodesmic shift of ca. 9 pH units in our calculated values would place our calculated values in excellent agreement with the "experimental" ones. Applying this relative shift to our pK_a values to align them with those derived from experiment would not affect any of our results or conclusions, but simply change the values of pH at which various processes occur.

Consistency check of calculated reduction potentials.

For the reaction

$$Co^{II}(dmgBF_2)_2^{0} + e^{-} \rightarrow Co^{I}(dmgBF_2)_2^{1-} \qquad \text{(S1)}$$

the reduction potential, given by the Nernst equation, is

$$E(\mathbf{Co}^{\mathrm{II}}/\mathrm{Co}^{\mathrm{I}}) = E^{\mathrm{o}}(\mathbf{Co}^{\mathrm{II}}/\mathbf{Co}^{\mathrm{I}}) + RT\ln([\mathbf{Co}^{\mathrm{II}}]/[\mathbf{Co}^{\mathrm{I}}]) \tag{S2}$$

where, for simplicity, we refer to $\mathrm{Co}^{\mathrm{II}}(\mathrm{dmgBF_2})_2^{\,0}$ as $\mathbf{Co}^{\mathrm{II}}$, etc.

In the presence of acid, the $\mathrm{Co}^{\mathrm{I}}(\mathrm{dmgBF_2})_2^{\,1-}$ may react with a proton to form $\mathrm{Co}^{\mathrm{III}}\mathrm{H}(\mathrm{dmgBF_2})_2^{\,0}$. The acid dissociation reaction of $\mathrm{Co}^{\mathrm{III}}\mathrm{H}(\mathrm{dmgBF_2})_2^{\,0}$,

$$\mathrm{Co}^{\mathrm{III}}\mathrm{H}(\mathrm{dmgBF_2})_2^{\,0} \rightarrow \mathrm{H}^+ + \mathrm{Co}^{\mathrm{I}}(\mathrm{dmgBF_2})_2^{\,1-} \tag{S3}$$

has $\mathrm{p}K_{\mathrm{a1}}$. If the reduction of $\mathrm{Co}^{\mathrm{II}}(\mathrm{dmgBF_2})_2^{\,0}$ is coupled to the protonation of $\mathrm{Co}^{\mathrm{I}}(\mathrm{dmgBF_2})_2^{\,1-}$, the reduction potential for the PCET process can be derived from eq. (S2) using $[\mathbf{Co}^{\mathrm{I}}] = K_{\mathrm{a1}}[\mathbf{Co}^{\mathrm{III}}\mathrm{H}]/[\mathrm{H}^+]$ as

$$\begin{aligned} E(\mathbf{Co}^{\mathrm{II}}/\mathbf{Co}^{\mathrm{III}}\mathrm{H}) &= E^{\mathrm{o}}(\mathbf{Co}^{\mathrm{II}}/\mathbf{Co}^{\mathrm{I}}) + RT\ln([\mathbf{Co}^{\mathrm{II}}][\mathrm{H}^+]/K_{\mathrm{a1}}[\mathbf{Co}^{\mathrm{III}}\mathrm{H}]) \\ &= E^{\mathrm{o}}(\mathbf{Co}^{\mathrm{II}}/\mathbf{Co}^{\mathrm{I}}) + RT\ln(10)\cdot\{\log([\mathrm{H}^+]) - \log(K_{\mathrm{a1}})\} \\ &\quad + RT\ln([\mathbf{Co}^{\mathrm{II}}]/[\mathbf{Co}^{\mathrm{III}}\mathrm{H}]) \\ &= E^{\mathrm{o}}(\mathbf{Co}^{\mathrm{II}}/\mathbf{Co}^{\mathrm{I}}) + RT\ln(10)\cdot(\mathrm{p}K_{\mathrm{a1}} - \mathrm{pH}) \\ &\quad + RT\ln([\mathbf{Co}^{\mathrm{II}}]/[\mathbf{Co}^{\mathrm{III}}\mathrm{H}]) \end{aligned} \tag{S4}$$

so that the half-potential for the $\mathbf{Co}^{\mathrm{II}}/\mathbf{Co}^{\mathrm{III}}\mathrm{H}$ couple would be

$$E_{1/2}(\mathbf{Co}^{\mathrm{II}}/\mathbf{Co}^{\mathrm{III}}\mathrm{H}) = E^{\mathrm{o}}(\mathbf{Co}^{\mathrm{II}}/\mathbf{Co}^{\mathrm{I}}) + RT\ln(10)\cdot(\mathrm{p}K_{\mathrm{a1}} - \mathrm{pH}) \tag{S5}$$

When $\mathrm{pH} = \mathrm{p}K_{\mathrm{a1}}$, the PCET half-potential is the same as that for the $\mathbf{Co}^{\mathrm{II}}/\mathbf{Co}^{\mathrm{I}}$ couple, but under standard conditions (i.e., pH 0) it is $E^{\mathrm{o}}(\mathbf{Co}^{\mathrm{II}}/\mathbf{Co}^{\mathrm{I}}) + RT\ln(10)\cdot\mathrm{p}K_{\mathrm{a1}}$ which is more positive than the $\mathbf{Co}^{\mathrm{II}}/\mathbf{Co}^{\mathrm{I}}$ couple unless $\mathrm{p}K_{\mathrm{a1}}$ is negative.

The calculated value of $E^{\mathrm{o}}(\mathbf{Co}^{\mathrm{II}}/\mathbf{Co}^{\mathrm{I}})$ is –0.946 V vs. NHE and the calculated value of $\mathrm{p}K_{\mathrm{a1}}$ is 4.47 so that $E^{\mathrm{o}}(\mathbf{Co}^{\mathrm{II}}/\mathbf{Co}^{\mathrm{III}}\mathrm{H})$ should be –0.681 V vs. NHE. The directly computed value of $E^{\mathrm{o}}(\mathbf{Co}^{\mathrm{II}}/\mathrm{Co}^{\mathrm{III}}\mathrm{H})$ is indeed –0.681 V vs. NHE.

The $\mathbf{Co}^{\mathrm{III}}\mathrm{H}/\mathbf{Co}^{\mathrm{II}}\mathrm{H}$ couple is related to the $\mathbf{Co}^{\mathrm{I}}/\mathbf{Co}^{0}$ couple through similar acid/base equilibria involving both members of the couple. In this case we must consider $\mathrm{p}K_{\mathrm{a2}}$ corresponding to the acid dissociation reaction of $\mathbf{Co}^{\mathrm{II}}\mathrm{H}$

$$\mathrm{Co}^{\mathrm{II}}\mathrm{H}(\mathrm{dmgBF_2})_2^{\,1-} \rightarrow \mathrm{H}^+ + \mathrm{Co}^{0}(\mathrm{dmgBF_2})_2^{\,2-} \tag{S6}$$

as well as $\mathrm{p}K_{\mathrm{a1}}$. Starting with the Nernst equation for the $\mathbf{Co}^{\mathrm{I}}/\mathbf{Co}^{0}$ couple, we substitute for both $[\mathbf{Co}^{\mathrm{I}}]$ and $[\mathbf{Co}^{0}]$ in terms of K_{a1} and K_{a2},

$$\begin{aligned} E(\mathbf{Co}^{\mathrm{III}}\mathrm{H}/\mathbf{Co}^{\mathrm{II}}\mathrm{H}) &= E^{\mathrm{o}}(\mathbf{Co}^{\mathrm{I}}/\mathbf{Co}^{0}) + RT\ln(K_{\mathrm{a1}}[\mathbf{Co}^{\mathrm{III}}\mathrm{H}][\mathrm{H}^+]/K_{\mathrm{a2}}[\mathbf{Co}^{\mathrm{II}}\mathrm{H}][\mathrm{H}^+]) \\ &= E^{\mathrm{o}}(\mathbf{Co}^{\mathrm{I}}/\mathbf{Co}^{0}) + RT\ln(10)\cdot\{\log(K_{\mathrm{a1}}) - \log(K_{\mathrm{a2}})\} \\ &\quad + RT\ln([\mathbf{Co}^{\mathrm{III}}\mathrm{H}]/[\mathbf{Co}^{\mathrm{II}}\mathrm{H}]) \\ &= E^{\mathrm{o}}(\mathbf{Co}^{\mathrm{I}}/\mathbf{Co}^{0}) + RT\ln(10)\cdot(\mathrm{p}K_{\mathrm{a2}} - \mathrm{p}K_{\mathrm{a1}}) \end{aligned} \tag{S7}$$

$$+\ RT\ln([\mathbf{Co}^{III}\mathrm{H}]/[\mathbf{Co}^{II}\mathrm{H}])$$

so that

$$E_{1/2}(\mathbf{Co}^{III}\mathrm{H}/\mathbf{Co}^{II}\mathrm{H}) = E^{o}(\mathbf{Co}^{I}/\mathbf{Co}^{0}) + RT\ln(10)\cdot(\mathrm{p}K_{a2} - \mathrm{p}K_{a1}) \qquad \text{(S8)}$$

independent of pH (provided that pH < pK_{a1} so that the oxidized species of the couple is $\mathbf{Co}^{III}$H). Note that since pK_{a2} is (considerably) larger than pK_{a1} (i.e., $\mathbf{Co}^{0}$ is much more basic than $\mathbf{Co}^{I}$), the shift in the half-potential of the $\mathbf{Co}^{III}$H/$\mathbf{Co}^{II}$H couple from the $\mathbf{Co}^{I}$/$\mathbf{Co}^{0}$ couple is positive. The calculated value of the $\mathbf{Co}^{I}$/$\mathbf{Co}^{0}$ couple is –1.381 V vs. NHE, and of pK_{a2} is 13.62 (see Fig. S5). This predicts a value of –0.840 V vs. NHE for $E_{1/2}(\mathbf{Co}^{III}\mathrm{H}/\mathbf{Co}^{II}\mathrm{H}) = E^{o}(\mathbf{Co}^{III}\mathrm{H}/\mathbf{Co}^{II}\mathrm{H})$. The directly computed value of $E^{o}(\mathbf{Co}^{III}\mathrm{H}/\mathbf{Co}^{II}\mathrm{H})$ is –0.840 V vs. NHE.

These results don't prove that the calculations are correct, but only that they are logically consistent.

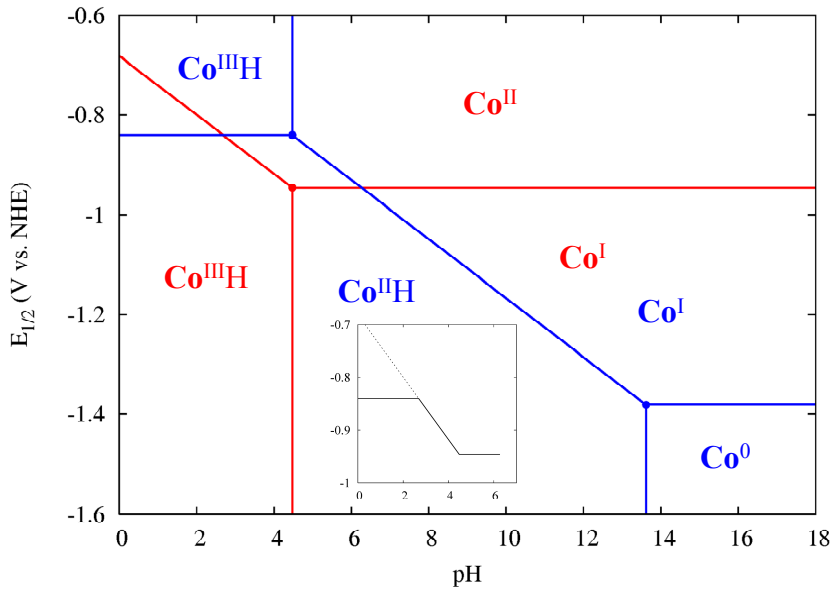

Fig. S4. Calculated Pourbaix (potential vs. pH) diagram for the electrochemical reduction of $\mathbf{Co}^{II}$. The calculations indicate that the thermodynamic limit for the catalytic production of H_2 by proton attack on $\mathbf{Co}^{II}$H (see inset) should reflect three distinct regions of the diagram. For 4.47 < pH < 6.27, it should be possible to make $\mathbf{Co}^{II}$H directly at the potential of the $\mathbf{Co}^{II}$/$\mathbf{Co}^{I}$ couple without making a $\mathbf{Co}^{III}$H intermediate; for 2.68 < pH < 4.47, it should become possible to make the $\mathbf{Co}^{III}$H intermediate via the $\mathbf{Co}^{II}$/$\mathbf{Co}^{III}$H PCET couple and immediately form $\mathbf{Co}^{II}$H by the $\mathbf{Co}^{III}$H/$\mathbf{Co}^{II}$H couple; and for pH < 2.68 (where the diagonal red line crosses the horizontal blue line), the potential for the formation of $\mathbf{Co}^{II}$H should become constant with decreasing pH, but that for the formation of $\mathbf{Co}^{III}$H should continue to become more positive. In this last case, the onset potential for the production of H_2 via $\mathbf{Co}^{II}$H should be constant at –0.840 V vs. NHE. The red and blue species with the same label, e.g., $\mathbf{Co}^{III}$H, are the same, but are involved in different redox couples. For comparison to the reported experimental pH scale, add 9 to the numbers on the abscissa.

Table S1. Calculated absolute standard free energies and free-energy differences for system and reservoir species involved in the proposed mechanisms for H_2 production by $\mathbf{Co^{II}}$.

Free Energy Profiles (System & Reservior) Large Basis	**Reservoir**	**System *G***	**Reservoir *G***	**Total *G***	**Δ*G* (eV)**	**Δ*G* *vs.* NHE (eV)**	**Cum. Δ*G* *vs.* NHE**
Protonation of $\mathbf{Co^{II}H}$ Mechanism							
$[\mathbf{Co^{II}}]^0$	$2H^+, 2e^-$	−2929.860149	−0.852156	−2930.712305	0.0000	0.0000	0.0000
$[\mathbf{Co^{I}}]^{1-}$	$2H^+, e^-$	−2929.991200	−0.850773	−2930.841972	−3.5284	0.9457	0.9457
$[\mathbf{Co^{III}}H]^0$	H^+, e^-	−2930.425620	−0.426078	−2930.851698	−0.2647	−0.2647	0.6810
$[\mathbf{Co^{II}}H]^{1-}$	H^+	−2930.560552	−0.424695	−2930.985247	−3.6341	0.8401	1.5211
$[\mathbf{Co^{II}}]^0$	H_2	−2929.860149	−1.180998	−2931.041147	−1.5211	−1.5211	0.0000
Homolysis of $\mathbf{Co^{III}H}$ Mechanism							
2 $[\mathbf{Co^{II}}]^0$	$2H^+, 2e^-$	−5859.720298	−0.852156	−5860.572454	0.0000	0.0000	0.0000
2 $[\mathbf{Co^{I}}]^{1-}$	$2H^+$	−5859.982399	−0.849389	−5860.831788	−7.0569	1.8914	1.8914
2 $[\mathbf{Co^{III}}H]^0$		−5860.851240	0.000000	−5860.851240	−0.5293	−0.5293	1.3621
2 $[\mathbf{Co^{II}}]^0$	H_2	−5859.720298	−1.180998	−5860.901295	−1.3621	−1.3621	0.0000
Protonation of $\mathbf{Co^{III}H}$ Mechanism							
$[\mathbf{Co^{II}}]^0$	$2H^+, 2e^-$	−2929.860149	−0.852156	−2930.712305	0.0000	0.0000	0.0000
$[\mathbf{Co^{I}}]^{1-}$	$2H^+, e^-$	−2929.991200	−0.850773	−2930.841972	−3.5284	0.9457	0.9457
$[\mathbf{Co^{III}}H]^0$	H^+, e^-	−2930.425620	−0.426078	−2930.851698	−0.2647	−0.2647	0.6810
$[\mathbf{Co^{III}}]^{1+}$	H_2, e^-	−2929.672411	−1.182381	−2930.854792	−0.0842	−0.0842	0.5968
$[\mathbf{Co^{II}}]^0$	H_2	−2929.860149	−1.180998	−2931.041147	−5.0710	−0.5968	0.0000
pK_a of $\mathbf{Co^{III}}H$				4.47			
pK_a of $\mathbf{Co^{II}}H$				13.62			

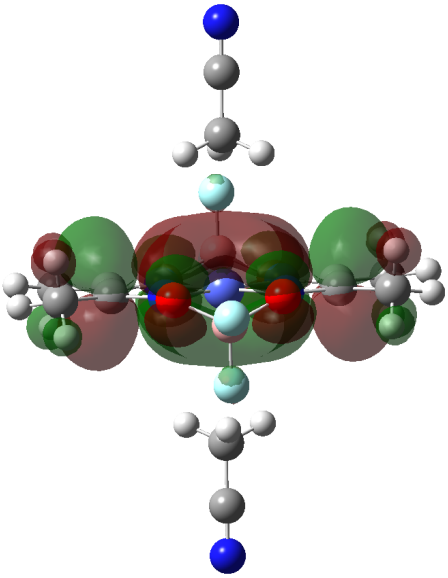

Fig. S5. Singly-occupied molecular orbital (SOMO, orbital 120α) of doublet **Co**^{0}. It is clear that this species is not strictly in oxidation state zero because the electron in this orbital is delocalized over the dmgBF$_2$ ligands thus imparting unusual stability to this low oxidation state and moving the standard potential of the **Co**^{I}/**Co**^{0} couple to an unexpectedly positive value (–1.379 V vs. NHE). The solvation free energy arising from the overall 2– charge of the complex also contributes to its stability.

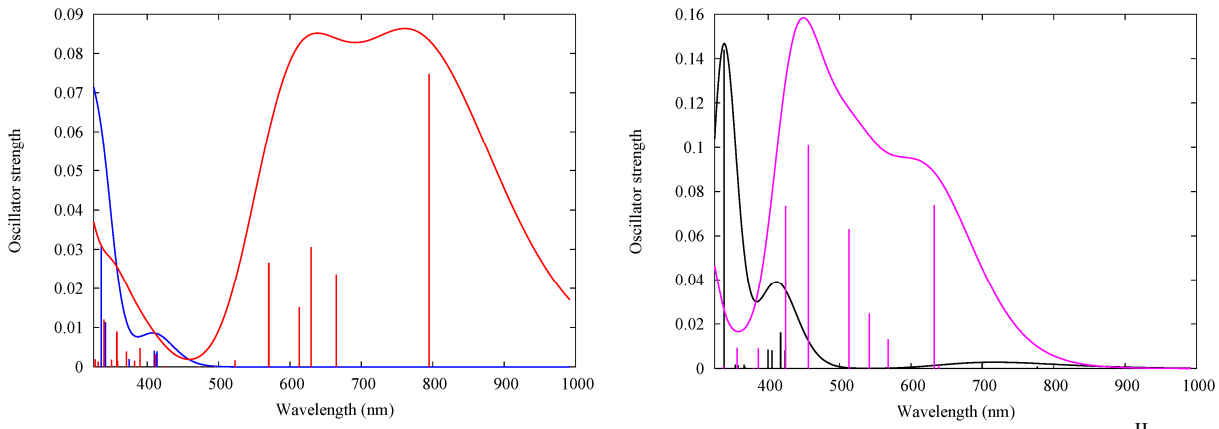

Fig. S6. Calculated UV-vis spectra of intermediates in hydrogen production using **Co**^{II} as a catalyst for possible identification via transient spectroscopy. Left panel: **Co**^{III}H (blue) and **Co**^{II}H (red). Right panel: **Co**^{II} (black) and **Co**^{I} (magenta). The spectra appear to be sufficiently different to allow identification of the intermediates. The spectra in the right panel match quite well with the initial and final time-dependent spectra reported by Hu et al.[17] for the oxidation of H$_2$ by **Co**^{II} in the presence of $CF_3CO_2^-$ to form an equilibrium mixture with CF_3COOH and **Co**^{I}.

Preliminary results on the calculation of transition states in the H_2 forming reactions in the three proposed mechanisms.

Preliminary work has been carried out to characterize any transition states in the hydrogen production steps of the three proposed reaction mechanisms. This section of the ESI summarizes our progress to date.

Proton attack on $Co^{III}H$ mechanism.

A gas-phase search for a transition state in the reaction between a proton and $\mathbf{Co}^{III}H$ to form H_2 and $\mathbf{Co}^{III}$ was carried out and resulted in the structure shown in Fig. S7. In the structure the incoming proton is interacting with both a glyoximate oxygen atom and the hydride bound to the Co(III) center. A subsequent vibrational frequency calculation resulted in a single imaginary frequency of 1523*i* cm^{-1} corresponding to the motion of the incoming proton between the glyoximate oxygen (H^+-O distance, 1.339 Å) and the hydride (H^+-H^- distance, 1.015 Å). The energetics of the formation of this structure in the gas phase are meaningless because the reactant proton is not solvated. A single-point calculation in a CPCM treatment of the acetonitrile solvent at the optimized gas-phase geometry predicts an activation free energy (with the small basis) of 2.55 eV.

When this structure was reoptimized in a CPCM treatment of the acetonitrile solvent, the transition state completely disappeared, presumably because of the ability of the dielectric continuum of the salvation model to stabilize charge separation. The ultimate optimized structure is shown in Fig. S8 and is a local minimum in the electronic energy corresponding to an η^2-H_2 adduct to the Co(III) center, i.e., a dihydrogen adduct (H-H distance, 0.787 Å, Co-H distances, 1.678 and 1.732 Å) that donates a pair of electrons into the same Co d orbital that bound the hydride ion. The free energy of this species is ca. –0.09 eV relative to reactants, but there is undoubtedly an activated step to reach this structure, and another one for it to lead to reaction products. The magnitude of the activation energy of this step is not clear, but it is most likely to be an activated process.

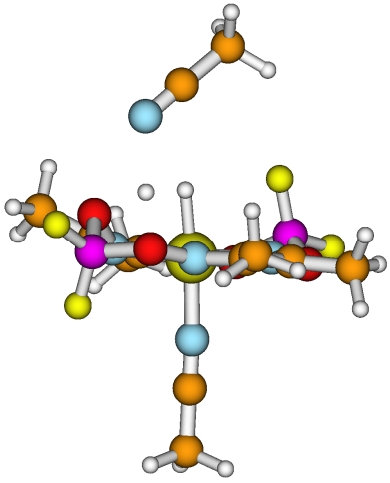

Fig. S7. Calculated gas-phase transition state structure in the reaction of a proton with **Co**^{III}H.

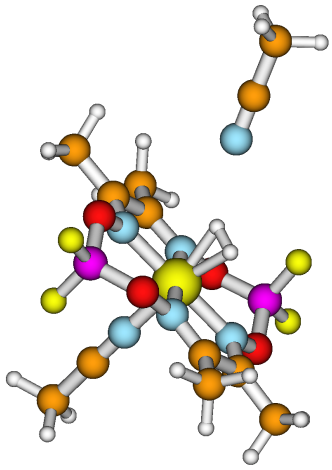

Fig. S8. Calculated solution-phase η^2-H_2 adduct intermediate in the reaction of a proton with **Co**^{III}H.

Homolysis of Co^{III}H mechanism.

The calculation of a transition state for the reaction of two **Co**^{III}H species to form H_2 and two **Co**^{II} complexes is difficult because it is large, and because it is further complicated by the two explicit solvent molecules in each reactant complex. An axial solvent molecule must be moved from the hydride side of each monomer to allow the two hydride ligands to approach each other closely enough to react. The equatorial glyoximate ligands hinder this approach, and (at least with the conformer considered here) require a very specific "lock and key" geometry involving the hydrogen atoms on the dmgBF$_2$ ligands on one reactant with the fluorine atoms of the dmgBF$_2$ ligands on the other reactant, and vice versa, as shown in Fig. S9 from a failed transition state search in acetonitrile solution. The electronic energy of the structure in Fig. S9, which is not yet at a transition state, is ca. 0.53 eV above that of reactants while the two hydride ligands are still separated by 1.715 Å. Moreover, the standard entropy change from reactants would be expected to have a very large negative value, contributing further to a large free energy of activation.

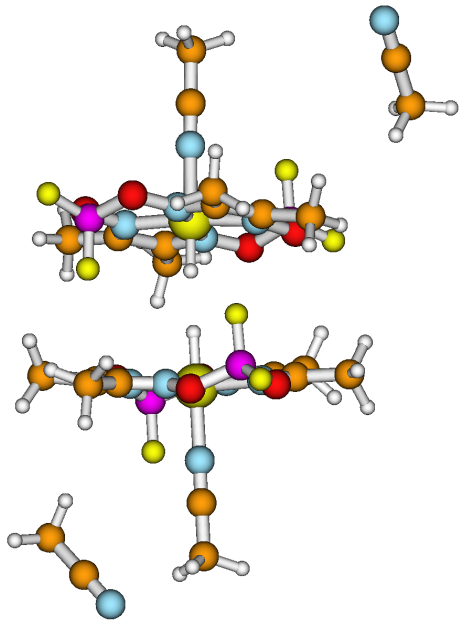

Fig. S9. Approaching a transition state for the homolysis of two **Co**^{III}H species to form H_2 and two **Co**^{II} complexes in acetonitrile solution. The dmgBF_2 ligands on the two reactant complexes cannot approach each other more closely without significantly increasing the electronic energy, and they have had to adopt a "lock and key" geometry in which the B-F bond of one reactant is positioned across from the methyl groups of other, and vice versa.

The hindered close approach of the two reactant complexes might be alleviated to some extent if the starting **Co**^{II} complexes were in the alternative conformation shown in Fig. S10, which is 2.41 kcal/mol less stable than the conformer considered in this work in the gas phase, but 3.26 kcal/mol more stable in acetonitrile solution. Because the stabilization of the electronic energy provided by the formation of the incipient H-H bond in the homolysis reaction would not be expected to occur until the H-H distance was rather short, and because the Co-H bonds must be stretched quite a lot to allow for such a close approach, it is most likely that the homolysis reaction is an activated process.

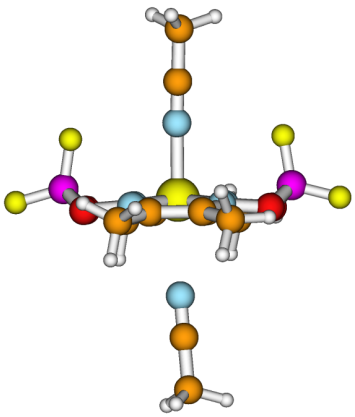

Fig. S10. Calculated structure of alternative conformation of the starting **Co**^{II} complex.

Proton attack on $Co^{II}H$ mechanism.

The interaction of a proton with $\mathbf{Co}^{II}H$, a complex with a single negative charge, is expected to be more attractive than that of a proton with the charge neutral $\mathbf{Co}^{III}H$ complex on the reactant side of the potential energy surface. This expectation is borne out in the structure of a stable proton adduct to $\mathbf{Co}^{II}H$ in the gas phase shown in Fig. S11 that is analogous to the gas-phase transition state for the H^+ + $\mathbf{Co}^{III}H$ reaction shown in Fig. S7. In this adduct, the Co-H^- bond distance is 1.722 Å, the O-H^+ bond distance is 1.098 Å, and the H^+-H^- distance is 1.346 Å. As in the case of the protonation of $\mathbf{Co}^{III}H$, a solution-phase search for a transition state in the reaction of a proton with $\mathbf{Co}^{II}H$ starting at the geometry of the gas-phase adduct in the H^+ + $\mathbf{Co}^{II}H$ reaction resulted in the structure shown in Fig. S11. This structure is far on the product side of the reaction potential energy surface, ca. −1.36 eV below reactants with an H_2 molecule having a bond distance of 0.749 Å and Co-H distances of 3.660 and 3.665 Å. The only sense in which this structure is a transition state is that the outgoing H_2 molecule and the incoming CH_3CN molecule that will take the place vacated by the hydride ion in the Co(II) coordination sphere manoeuvre around each other at some small expense in electronic energy. It thus appears that the protonation of $\mathbf{Co}^{II}H$ is not an activated process, and it is the most likely mechanism for H_2 production with the $\mathbf{Co}^{II}$ electrocatalyst.

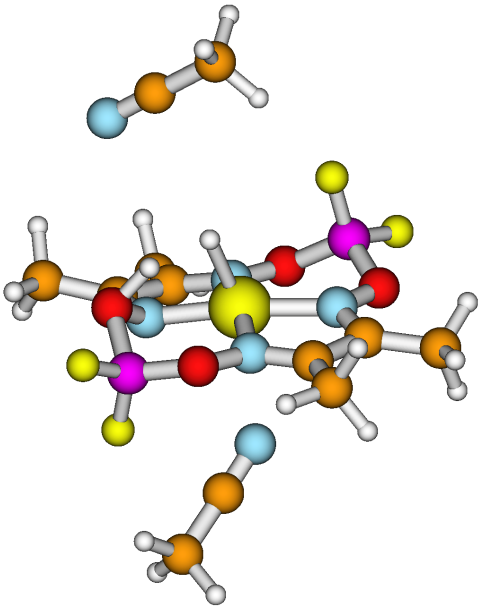

Fig. S11. Calculated structure of a proton adduct intermediate in the gas-phase reaction of a proton with $\mathbf{Co}^{II}H$.

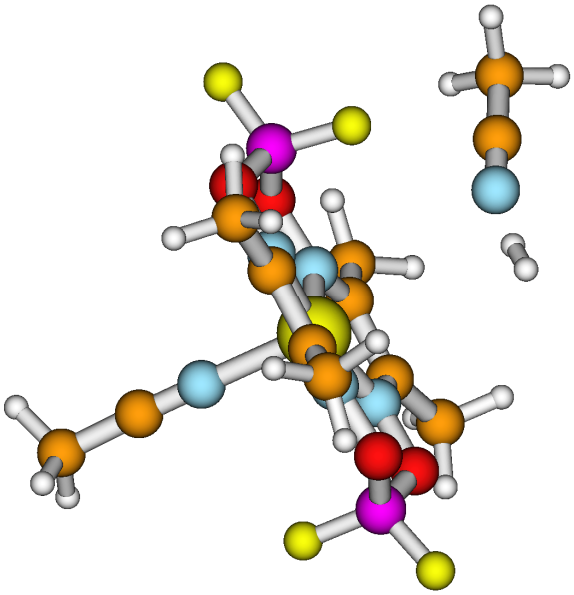

Fig. S12. Calculated structure of a product-like "transition state" in the reaction of a proton with $\mathbf{Co}^{II}H$.

Cartesian coordinates of optimized structures of key species.

$[Co^{III}(dmgBF_2)_2{\cdot}2CH_3CN]^{1+}$, **$Co^{III}$**

Co	0.001159	-0.000266	0.000619
N	1.171462	1.432001	0.485019
N	-1.164497	1.453097	-0.429024
N	-1.169158	-1.432530	-0.483759
N	1.166803	-1.453625	0.430283
C	1.410522	-3.900120	0.590564
H	1.008899	-4.331142	1.516272
H	2.468621	-3.688223	0.745751
H	1.295432	-4.648306	-0.198568
C	0.680054	-2.644219	0.240385
C	-1.420848	-3.870470	-0.736227
H	-2.477915	-3.649091	-0.885010
H	-1.309770	-4.647549	0.025093
H	-1.019272	-4.268744	-1.676501
C	-0.686319	-2.631039	-0.339020
C	1.423142	3.869935	0.737528
H	2.480227	3.648576	0.886211
H	1.021635	4.268124	1.677868
H	1.311979	4.647069	-0.023723
C	-1.408222	3.899599	-0.589266
H	-1.293270	4.647701	0.199968
H	-2.466290	3.687682	-0.744623
H	-1.006474	4.330743	-1.514863
C	0.688620	2.630510	0.340290
C	-0.677752	2.643690	-0.239118
O	2.342209	1.233412	1.094021
O	2.338121	-1.282086	1.046403
O	-2.339921	-1.233939	-1.092738
O	-2.335834	1.281560	-1.045119
B	-3.115371	0.017825	-0.684961
F	-3.312269	-0.007914	0.690336
F	-4.233957	0.034069	-1.447590
B	3.117661	-0.018347	0.686230
F	3.314510	0.007391	-0.689064
F	4.236258	-0.034594	1.448842
C	1.120860	0.051565	-2.833080
N	0.644010	0.032562	-1.785222
C	-1.118966	-0.052125	2.834126
N	-0.641780	-0.033109	1.786421
C	1.760528	0.075201	-4.137559
H	1.462446	-0.804681	-4.714886
H	1.465140	0.977125	-4.681279
H	2.846104	0.070910	-3.997575
C	-1.759150	-0.075737	4.138351
H	-1.460683	0.803742	4.716094
H	-2.844664	-0.070649	3.997904
H	-1.464617	-0.978047	4.681893

$[Co^{II}(dmgBF_2)_2{\cdot}2CH_3CN]^0$, **Co**^{II}

Co	0.001205	-0.000466	0.000459
N	1.229436	1.420190	0.299613
N	-1.216480	1.439561	-0.243885
N	-1.227065	-1.421124	-0.298429
N	1.218740	-1.440504	0.245228
C	1.475367	-3.892128	0.399206
H	1.204897	-4.318572	1.373687
H	2.544610	-3.677700	0.408627
H	1.258634	-4.646651	-0.363135
C	0.708900	-2.632637	0.140119
C	-1.501737	-3.863339	-0.544922
H	-2.569163	-3.640013	-0.550487
H	-1.294016	-4.646036	0.191114
H	-1.230759	-4.257391	-1.532795
C	-0.726130	-2.620141	-0.238617
C	1.504126	3.862395	0.545980
H	2.571579	3.639166	0.550859
H	1.233732	4.256133	1.534139
H	1.295894	4.645280	-0.189705
C	-1.473113	3.891210	-0.397556
H	-1.256541	4.645502	0.365062
H	-2.542342	3.676733	-0.407208
H	-1.202498	4.317989	-1.371851
C	0.728467	2.619193	0.239809
C	-0.706610	2.631678	-0.138741
O	2.497909	1.248744	0.721986
O	2.488309	-1.294706	0.673850
O	-2.495457	-1.249620	-0.721090
O	-2.486139	1.293826	-0.672293
B	-3.191894	0.016599	-0.276421
F	-3.333972	-0.009728	1.121322
F	-4.392540	0.033782	-0.941107
B	3.194212	-0.017673	0.277560
F	3.336181	0.008234	-1.120163
F	4.394887	-0.034790	0.942192
C	1.232874	0.055758	-3.132563
N	0.442001	0.042027	-2.286524
C	-1.230921	-0.055320	3.133959
N	-0.439145	-0.042023	2.288738
C	2.271560	0.071777	-4.153942
H	2.181910	-0.805569	-4.800513
H	2.189108	0.974543	-4.765505
H	3.242931	0.057811	-3.650657
C	-2.270442	-0.070780	4.154515
H	-2.180837	0.806489	4.801180
H	-3.241418	-0.056555	3.650496
H	-2.188849	-0.973617	4.766108

$[Co^{I}(dmgBF_2)_2{\cdot}2CH_3CN]^{1-}$, **Co**^{I}

Co	0.127153	-0.066724	-0.343063
N	0.444890	-1.823569	0.107651
N	-1.105603	-0.191913	1.018442
N	0.138433	1.772541	-0.397698
N	1.668807	0.139801	-1.325962
C	3.119903	1.649236	-2.651356
H	2.940178	1.220090	-3.646715
H	4.034818	1.177472	-2.273723
H	3.299262	2.722080	-2.766595
C	1.968535	1.382748	-1.724506
C	1.141476	3.840543	-1.332608
H	0.171632	4.232173	-1.663172
H	1.902739	4.125497	-2.064536
H	1.369059	4.346968	-0.384295
C	1.077851	2.349510	-1.163398
C	-0.305276	-3.831293	1.348068
H	0.709111	-4.096261	1.671305
H	-0.523432	-4.460300	0.474970
H	-1.006218	-4.091788	2.146367
C	-2.275432	-1.637500	2.662718
H	-2.418761	-2.704575	2.856017
H	-3.245576	-1.189661	2.417995
H	-1.950800	-1.161346	3.599624
C	-0.385878	-2.371855	1.002113
C	-1.287349	-1.409054	1.554481
O	1.303927	-2.690827	-0.541529
O	2.423984	-0.881338	-1.874735
O	-0.714990	2.640589	0.258427
O	-1.884675	0.820559	1.547480
B	-1.983576	2.072826	0.758019
F	-2.892646	1.882511	-0.333458
F	-2.525214	3.034100	1.632087
B	2.569747	-2.076064	-1.008954
F	3.390857	-1.752322	0.120470
F	3.212729	-3.050902	-1.790496
C	3.835415	1.173202	3.043249
N	4.643270	1.502979	3.814173
C	-6.088664	-0.777053	-0.971236
N	-7.236948	-0.892972	-1.122985
C	2.818500	0.760184	2.078990
H	2.610283	1.565967	1.369284
H	3.141090	-0.119703	1.510730
H	1.882952	0.518733	2.590952
C	-4.646607	-0.645612	-0.785775
H	-4.115755	-0.921085	-1.701575
H	-4.353156	0.379042	-0.529768
H	-4.306114	-1.305837	0.016973
C	-1.032623	-0.525383	-1.898705
H	-1.742490	-1.300065	-1.581638
H	-1.570444	0.371103	-2.225036
H	-0.398899	-0.917218	-2.701910

$[Co^0(dmgBF_2)_2{\cdot}2CH_3CN]^{2-}$, **Co**^{0}

C	0.201246	0.623022	0.268200
C	0.220112	0.199041	1.708021
C	1.368661	-0.225392	2.465243
C	2.771789	-0.381547	1.955377
N	-0.892066	0.194936	2.452315
O	-2.051990	0.653561	1.845748
B	-3.311207	0.136483	2.438675
F	-4.351278	0.832039	1.795540
Co	-0.719620	-0.308026	4.217754
N	1.049405	-0.500688	3.735379
O	2.065131	-0.989157	4.543840
B	1.871933	-0.753235	5.996866
F	2.911855	-1.449297	6.639732
N	-2.488637	-0.115328	4.700146
O	-3.504356	0.373028	3.891617
N	-0.547226	-0.811147	5.983157
O	0.612599	-1.270377	6.589495
C	-2.807917	-0.390616	5.970279
C	-1.659411	-0.815188	6.727487
C	-1.640709	-1.239650	8.167173
C	-4.211031	-0.234336	6.480145
F	1.991657	0.648092	6.274266
F	-3.430657	-1.265022	2.161975
C	-1.547774	-3.638188	3.264587
C	-1.837639	-5.025076	2.906593
N	-2.064277	-6.131673	2.624059
C	0.104510	3.020917	5.179624
C	0.388842	4.407719	5.542316
N	0.611175	5.514219	5.828629
H	-0.007067	1.697846	0.163344
H	-0.599361	0.102938	-0.271361
H	1.154762	0.410278	-0.224368
H	3.479558	0.110917	2.632814
H	2.884320	0.046809	0.954901
H	3.073916	-1.438282	1.912126
H	-4.918777	-0.728336	5.803776
H	-4.513624	0.822321	6.521556
H	-4.323112	-0.661014	7.481382
H	-2.593193	-1.024168	8.660558
H	-0.838094	-0.722073	8.706102
H	-1.435614	-2.315147	8.271715
H	-0.547820	-3.354817	2.924679
H	-2.271513	-2.947848	2.816300
H	-1.576595	-3.507288	4.349822
H	0.137317	2.893054	4.094146
H	0.829024	2.331672	5.628328
H	-0.895622	2.733300	5.515411

$[Co^{III}H(dmgBF_2)_2{\cdot}2CH_3CN]^0$, **$Co^{III}H$**

Co	0.034468	0.169170	0.274926
N	-0.066096	-0.350953	2.095290
N	1.883962	-0.095798	0.569901
N	0.160276	0.894115	-1.465736
N	-1.785758	0.653645	0.065014
C	-3.445898	1.783093	-1.379424
H	-3.397655	2.878664	-1.375316
H	-4.173195	1.455058	-0.636952
H	-3.771364	1.468070	-2.376033
C	-2.096802	1.224366	-1.061670
C	-1.076458	1.850162	-3.382495
H	-0.094035	1.913064	-3.849878
H	-1.535025	2.843461	-3.359127
H	-1.714515	1.195374	-3.988297
C	-0.949687	1.318336	-1.991310
C	1.186632	-0.985163	4.119954
H	0.253199	-1.432171	4.466445
H	1.369927	-0.090248	4.728432
H	2.013371	-1.680170	4.286007
C	3.631213	-0.803152	2.162800
H	3.857944	-0.365530	3.139705
H	4.321466	-0.407676	1.417247
H	3.790342	-1.886060	2.238957
C	1.068692	-0.623978	2.672377
C	2.222390	-0.498319	1.759703
O	-1.186858	-0.338584	2.833560
O	-2.705339	0.574742	1.044759
O	1.286783	0.852543	-2.207190
O	2.817303	-0.005107	-0.394784
B	2.571573	1.056471	-1.446027
F	2.539901	2.309189	-0.816170
F	3.583756	0.919923	-2.359771
B	-2.491835	-0.502133	2.077295
F	-2.498131	-1.755697	1.453488
F	-3.483787	-0.342358	3.008020
C	-0.550567	-2.773290	-0.712667
N	-0.235901	-1.701661	-0.424641
C	-0.280404	4.953649	-0.988817
N	-1.337475	4.725670	-1.413398
C	-0.989727	-4.120846	-1.044339
H	-1.232807	-4.185838	-2.108488
H	-0.200582	-4.841855	-0.813969
H	-1.880003	-4.356220	-0.453429
C	1.054140	5.222895	-0.460531
H	0.988154	5.497617	0.596220
H	1.676571	4.328395	-0.562950
H	1.514448	6.047581	-1.012463
H	0.214904	1.509448	0.778790

$[Co^{II}H(dmgBF_2)_2{\cdot}2CH_3CN]^{1-}$, **Co**^{II}H

Co	0.118284	0.529284	0.427947
N	-0.015787	-0.244754	2.118804
N	1.916951	0.083776	0.633853
N	0.224383	1.076593	-1.355387
N	-1.709287	0.763766	0.138247
C	-3.466674	1.577315	-1.406123
H	-3.681827	2.631930	-1.187964
H	-4.158816	0.970027	-0.819220
H	-3.648000	1.415868	-2.472386
C	-2.056070	1.230262	-1.041694
C	-1.027194	1.876585	-3.350134
H	-0.031013	2.033117	-3.764744
H	-1.585984	2.817647	-3.399542
H	-1.551208	1.143371	-3.977055
C	-0.914203	1.397778	-1.934181
C	1.184390	-1.206226	4.056059
H	0.220613	-1.643914	4.323938
H	1.402544	-0.418187	4.789900
H	1.965159	-1.967600	4.138027
C	3.668229	-0.840412	2.108993
H	3.820798	-0.912967	3.188428
H	4.350675	-0.093441	1.694502
H	3.940241	-1.804382	1.658780
C	1.111390	-0.649630	2.666514
C	2.254517	-0.463914	1.783336
O	-1.149937	-0.288020	2.870229
O	-2.673773	0.626094	1.088261
O	1.364451	1.122626	-2.099113
O	2.895204	0.251077	-0.296138
B	2.646740	1.297125	-1.342184
F	2.671661	2.574426	-0.746880
F	3.658809	1.143047	-2.275323
B	-2.413212	-0.465129	2.082605
F	-2.359866	-1.703805	1.401887
F	-3.448715	-0.411132	2.997041
C	-0.687248	-4.509628	-1.325803
N	-0.850946	-5.596768	-1.703385
C	-0.560135	5.325188	-1.308327
N	-1.301450	5.755040	-2.094234
C	-0.474688	-3.142187	-0.856642
H	-0.545940	-2.444140	-1.695804
H	-1.217824	-2.863114	-0.102925
H	0.523014	-3.047668	-0.418348
C	0.366221	4.783137	-0.318225
H	-0.146750	4.066287	0.330517
H	1.191789	4.249683	-0.799250
H	0.771103	5.593775	0.295263
H	0.270895	1.884088	1.000899

$[Co^{I}H(dmgBF_2)_2{\cdot}2CH_3CN]^{2-}$, **Co**^{I}H

Co	0.067700	0.669235	0.410466
N	-0.047316	-0.187639	2.033907
N	1.811253	0.091233	0.500601
N	0.107484	1.075146	-1.381788
N	-1.747817	0.802990	0.152320
C	-3.613373	1.448861	-1.344619
H	-4.003973	2.290390	-0.755551
H	-4.211808	0.574031	-1.063639
H	-3.780354	1.663717	-2.404079
C	-2.159575	1.205984	-1.057653
C	-1.149235	1.722383	-3.421578
H	-0.466500	2.548885	-3.655562
H	-2.164577	2.017083	-3.702043
H	-0.843834	0.885483	-4.065361
C	-1.069041	1.355671	-1.967423
C	1.142305	-1.278767	3.913512
H	0.319351	-1.989048	4.050181
H	1.020716	-0.511150	4.691895
H	2.089693	-1.796714	4.089283
C	3.606685	-0.959145	1.849067
H	3.740508	-1.398824	2.841624
H	4.291669	-0.107128	1.747771
H	3.922318	-1.695786	1.098370
C	1.091800	-0.679294	2.537923
C	2.185882	-0.524608	1.631463
O	-1.156148	-0.233804	2.858884
O	-2.725906	0.680126	1.123445
O	1.216995	1.128976	-2.205122
O	2.791208	0.230571	-0.461257
B	2.534685	1.222395	-1.531704
F	2.729471	2.545754	-1.027905
F	3.494963	0.968198	-2.529072
B	-2.452844	-0.352894	2.149355
F	-2.554824	-1.655408	1.557945
F	-3.449507	-0.205733	3.129376
C	-0.333672	-4.332850	-0.724943
N	-0.378391	-5.459564	-1.015268
C	0.303049	6.002073	-0.888436
N	0.298423	7.145537	-1.109051
C	-0.276075	-2.918387	-0.364183
H	-0.270319	-2.294694	-1.262320
H	-1.133091	-2.629365	0.254860
H	0.637391	-2.701535	0.197299
C	0.302468	4.570397	-0.603290
H	-0.494759	4.066259	-1.157558
H	1.253669	4.099335	-0.875727
H	0.133581	4.384427	0.461060
H	0.251185	2.019096	0.997544

$[Co^{III}Me(dmgBF_2)_2{\cdot}2CH_3CN]^0$, **Co**^{III}Me

Co	-0.326173	0.110073	-0.023269
N	-1.933498	0.440209	-0.972114
N	-0.242474	2.004484	-0.018344
N	1.312127	-0.215084	0.872220
N	-0.364681	-1.783041	-0.097073
C	0.887028	-3.869700	0.352525
H	1.737818	-4.083253	-0.305889
H	0.000478	-4.368390	-0.038746
H	1.126881	-4.272960	1.341793
C	0.660368	-2.393491	0.420419
C	2.796610	-1.938177	1.849564
H	3.383398	-1.086664	2.193117
H	3.425493	-2.584333	1.229316
H	2.467452	-2.516343	2.721314
C	1.618998	-1.464308	1.059487
C	-3.408332	2.143532	-1.978334
H	-4.140843	1.337705	-2.039684
H	-3.112701	2.409497	-3.001210
H	-3.868800	3.025949	-1.525088
C	-1.388989	4.107492	-0.616881
H	-1.707090	4.446004	-1.607429
H	-0.440780	4.579047	-0.356920
H	-2.145017	4.439147	0.106069
C	-2.221245	1.691178	-1.186751
C	-1.238946	2.618332	-0.587271
O	-2.692500	-0.519770	-1.526392
O	-1.291823	-2.484308	-0.776377
O	2.034656	0.750549	1.476934
O	0.672966	2.717137	0.662579
B	2.047420	2.097227	0.800226
F	2.616285	1.969452	-0.474516
F	2.748435	2.931581	1.633549
B	-2.671786	-1.874580	-0.842291
F	-3.178640	-1.732731	0.455624
F	-3.415608	-2.703662	-1.639055
C	-1.972951	-0.003514	2.680439
N	-1.293146	0.131860	1.758380
C	4.502373	-1.203067	-1.617676
N	4.166314	-2.266622	-1.292321
C	-2.859418	-0.209374	3.816391
H	-2.299062	-0.618122	4.661767
H	-3.315136	0.738457	4.115740
H	-3.644435	-0.914074	3.525891
C	4.909321	0.143305	-2.011348
H	4.806420	0.262712	-3.093807
H	4.275731	0.880229	-1.507153
H	5.953511	0.314243	-1.733932
C	0.558054	0.019439	-1.804370
H	0.651150	1.029899	-2.203452
H	1.546047	-0.423078	-1.679381
H	-0.062372	-0.604032	-2.450479

$[Co^{II}Me(dmgBF_2)_2{\cdot}2CH_3CN]^{1-}$, **Co**^{II}Me

Co	0.171076	0.040586	-0.207264
N	1.080831	-1.177148	-1.292034
N	-0.427368	-1.521421	0.624001
N	-0.504743	1.229873	1.065119
N	1.003220	1.584360	-0.849565
C	1.191819	4.049204	-0.691030
H	0.443610	4.566543	-1.306636
H	2.087903	3.917785	-1.300154
H	1.423720	4.692607	0.163181
C	0.694020	2.709061	-0.240152
C	-0.658957	3.577168	1.828923
H	-1.657377	3.330979	2.198554
H	-0.685945	4.545935	1.323551
H	-0.005105	3.669799	2.706711
C	-0.183864	2.496954	0.904652
C	1.405352	-3.553558	-1.910727
H	2.294004	-3.192414	-2.431585
H	0.685678	-3.884295	-2.671772
H	1.669373	-4.422619	-1.300568
C	-0.444173	-3.995202	0.615922
H	-0.434938	-4.755210	-0.169682
H	-1.445632	-3.929290	1.047991
H	0.230458	-4.327059	1.416820
C	0.838865	-2.451306	-1.067343
C	-0.038805	-2.655752	0.078627
O	1.823453	-0.839880	-2.381900
O	1.753967	1.645037	-1.983348
O	-1.252690	0.900231	2.153795
O	-1.181767	-1.589355	1.755452
B	-2.018364	-0.385989	2.071308
F	-3.040973	-0.261477	1.109194
F	-2.529402	-0.603826	3.340305
B	2.602187	0.433578	-2.234018
F	3.523529	0.288920	-1.171420
F	3.227878	0.645943	-3.448444
C	4.664501	-0.454594	2.846956
N	5.626791	-0.591418	3.484514
C	-6.713664	0.167741	-1.256246
N	-7.834011	0.421668	-1.434218
C	3.450887	-0.283954	2.051210
H	2.880831	0.574402	2.418250
H	3.690837	-0.120463	0.995759
H	2.819853	-1.173442	2.135268
C	-5.305271	-0.154869	-1.039715
H	-4.667778	0.480851	-1.660339
H	-5.014859	-0.010824	0.004237
H	-5.113990	-1.198622	-1.304393
C	-1.308368	0.214656	-1.544989
H	-1.891435	-0.709906	-1.537845
H	-1.938629	1.059477	-1.255130
H	-0.848830	0.382985	-2.522513

$[Co^{I}Me(dmgBF_2)_2{\cdot}2CH_3CN]^{2-}$, **Co**^{I}Me

Co	0.127153	-0.066724	-0.343063
N	0.444890	-1.823569	0.107651
N	-1.105603	-0.191913	1.018442
N	0.138433	1.772541	-0.397698
N	1.668807	0.139801	-1.325962
C	3.119903	1.649236	-2.651356
H	2.940178	1.220090	-3.646715
H	4.034818	1.177472	-2.273723
H	3.299262	2.722080	-2.766595
C	1.968535	1.382748	-1.724506
C	1.141476	3.840543	-1.332608
H	0.171632	4.232173	-1.663172
H	1.902739	4.125497	-2.064536
H	1.369059	4.346968	-0.384295
C	1.077851	2.349510	-1.163398
C	-0.305276	-3.831293	1.348068
H	0.709111	-4.096261	1.671305
H	-0.523432	-4.460300	0.474970
H	-1.006218	-4.091788	2.146367
C	-2.275432	-1.637500	2.662718
H	-2.418761	-2.704575	2.856017
H	-3.245576	-1.189661	2.417995
H	-1.950800	-1.161346	3.599624
C	-0.385878	-2.371855	1.002113
C	-1.287349	-1.409054	1.554481
O	1.303927	-2.690827	-0.541529
O	2.423984	-0.881338	-1.874735
O	-0.714990	2.640589	0.258427
O	-1.884675	0.820559	1.547480
B	-1.983576	2.072826	0.758019
F	-2.892646	1.882511	-0.333458
F	-2.525214	3.034100	1.632087
B	2.569747	-2.076064	-1.008954
F	3.390857	-1.752322	0.120470
F	3.212729	-3.050902	-1.790496
C	3.835415	1.173202	3.043249
N	4.643270	1.502979	3.814173
C	-6.088664	-0.777053	-0.971236
N	-7.236948	-0.892972	-1.122985
C	2.818500	0.760184	2.078990
H	2.610283	1.565967	1.369284
H	3.141090	-0.119703	1.510730
H	1.882952	0.518733	2.590952
C	-4.646607	-0.645612	-0.785775
H	-4.115755	-0.921085	-1.701575
H	-4.353156	0.379042	-0.529768
H	-4.306114	-1.305837	0.016973
C	-1.032623	-0.525383	-1.898705
H	-1.742490	-1.300065	-1.581638
H	-1.570444	0.371103	-2.225036
H	-0.398899	-0.917218	-2.701910

References

1. Gaussian03, Revision D.01, M. J. Frisch, G. W. Trucks, H. B. Schlegel, G. E. Scuseria, M. A. Robb, J. R. Cheeseman, J. A. Montgomery, Jr., T. Vreven, K. N. Kudin, J. C. Burant, J. M. Millam, S. S. Iyengar, J. Tomasi, V. Barone, B. Mennucci, M. Cossi, G. Scalmani, N. Rega, G. A. Petersson, H. Nakatsuji, M. Hada, M. Ehara, K. Toyota, R. Fukuda, J. Hasegawa, M. Ishida, T. Nakajima, Y. Honda, O. Kitao, H. Nakai, M. Klene, X. Li, J. E. Knox, H. P. Hratchian, J. B. Cross, V. Bakken, C. Adamo, J. Jaramillo, R. Gomperts, R. E. Stratmann, O. Yazyev, A. J. Austin, R. Cammi, C. Pomelli, J. W. Ochterski, P. Y. Ayala, K. Morokuma, G. A. Voth, P. Salvador, J. J. Dannenberg, V. G. Zakrzewski, S. Dapprich, A. D. Daniels, M. C. Strain, O. Farkas, D. K. Malick, A. D. Rabuck, K. Raghavachari, J. B. Foresman, J. V. Ortiz, Q. Cui, A. G. Baboul, S. Clifford, J. Cioslowski, B. B. Stefanov, G. Liu, A. Liashenko, P. Piskorz, I. Komaromi, R. L. Martin, D. J. Fox, T. Keith, M. A. Al-Laham, C. Y. Peng, A. Nanayakkara, M. Challacombe, P. M. W. Gill, B. Johnson, W. Chen, M. W. Wong, C. Gonzalez, and J. A. Pople, Gaussian, Inc., Wallingford CT, 2004.
2. A. D. Becke, *J. Chem. Phys.*, 1993, **98**, 5648-5652.
3. A. D. McLean and G. S. Chandler, *J. Chem. Phys.*, 1980, **72**, 5639-5648.
4. K. Raghavachari, J. S. Binkley, R. Seeger and J. A. Pople, *J. Chem. Phys.*, 1980, **72**, 650-654.
5. A. J. H. Wachters, *J. Chem. Phys.*, 1970, **52**, 1033.
6. P. J. Hay, *J. Chem. Phys.*, 1977, **66**, 4377-4384.
7. R. Ditchfield, W. J. Hehre and J. A. Pople, *J. Chem. Phys.*, 1971, **54**, 724.
8. M. M. Francl, W. J. Pietro, W. J. Hehre, J. S. Binkley, M. S. Gordon, D. J. Defrees and J. A. Pople, *J. Chem. Phys.*, 1982, **77**, 3654-3665.
9. W. J. Hehre, R. Ditchfield and J. A. Pople, *J. Chem. Phys.*, 1972, **56**, 2257-2261.
10. A. Klamt and G. Schuurmann, *J. Chem. Soc-Perkin Trans.*, 1993, **2**, 799-805.
11. V. Barone and M. Cossi, *J. Phys. Chem. A*, 1998, **102**, 1995-2001.
12. M. Cossi, N. Rega, G. Scalmani and V. Barone, 2003, **24**, 669-681.
13. A. Bondi, *J. Phys. Chem.*, 1964, **68**, 441-451.
14. C. P. Kelly, C. J. Cramer and D. G. Truhlar, *J. Phys. Chem. B*, 2007, **111**, 408-422.
15. J. E. Bartmess, *J. Phys. Chem.*, 1994, **98**, 6420-6424.
16. C. Baffert, V. Artero, M. Fontecave, *Inorg. Chem,*. 2007, **46**, 1817-1824.
17. X. Hu, B. S. Brunschwig and J. C. Peters, J. Am. Chem., Soc. 2007, **129**, 8988-8998.